Plasma Chem Plasma Process (2016) 36:1011–1020
DOI 10.1007/s11090-016-9714-5

ORIGINAL PAPER

Degradation of Organic Pollutants Using Atmospheric Pressure Glow Discharge Plasma

Wenzheng Liu[1] · Qiang zhao[1] · Tahan Wang[1] · Xiaoxia Duan[2] · Chuanhui Li[1] · Xiao Lei[1]

Received: 25 September 2015 / Accepted: 24 April 2016 / Published online: 30 April 2016

Abstract A method of plasma treatment in which a glow discharge was generated in the small gas gap between an electrode and a water surface was designed and employed in this study. By using this method, many active species were generated on the wastewater surface to degrade organic pollutants. The electric field distribution of the designed electrode model was simulated using the MAXWELL 3D® simulation software, and the discharge parameters were measured to investigate the impact of design optimization. In addition, we designed an equipotential multi-electrode configuration to treat a methyl orange solution and an azobenzene solution. The experimental and simulation results indicate that the designed electrodes can realize glow discharge with a relatively low voltage and that the generated plasma covers a large area and is in a stable state. Accordingly, the method helped reduce the cost of the reactor and improved the effectiveness of wastewater treatment.

Keywords Wastewater treatment · Water surface · Plasma · Glow discharge · Organic pollutants

Introduction

Traditional wastewater treatment methods leave residual organic pollutants that are difficult to effectively degrade in water [1–3]. However, an advanced oxidation process (AOP) can be used to effectively degrade residual organic pollutants and other pollutants [4–8]. AOPs include catalytic wet air oxidation [9–11], photochemical oxidation [12–14], and plasma oxidation, among others [15–18]. Among these methods, low-temperature plasma

✉ Wenzheng Liu
wzhliu@bjtu.edu.cn

[1] School of Electrical Engineering, Beijing Jiaotong University, Beijing 100044, China

[2] School of Science, Beijing Jiaotong University, Beijing 100044, China

technology is a type of wastewater treatment method that applies the effects of high-energy electrons, ozone oxidation, and ultraviolet radiation. Low-temperature plasma oxidation generates strong oxidation of active species which can act at the gas–liquid interface and make the residual organic pollutants degrade. The technique primarily includes bubbles in water, droplets in gas, and a plasma jet on the liquid surface [19–24].

Existing low-temperature plasma water treatment methods generally use corona discharge; most of these techniques require the use of aeration equipment or an atomizing device, resulting in low processing efficiency, increased investment in water treatment equipment, and power loss caused by an external device [25, 26]. This study proposes a new treatment method that can generate water surface glow discharge plasma in an atmospheric pressure air environment. The discharge electrodes are placed on the liquid surface. By taking advantage of the strong field strength in the small air gap between the electrode and the water surface, glow discharges were generated and used to treat wastewater. The luminous area and plasma density of glow discharge is larger than the corona discharge. Compared to existing corona plasma treatment method, this method produces high-density glow discharge plasma, a large contact area with the fluid, a reactor with a simple structure, and high treatment efficiency. The results may lead to a new wastewater treatment method.

Results and Discussion

A structural diagram of the designed electrode model is shown in Fig. 1. In this study, a dielectric barrier discharge (DBD) in which the dielectric is composed primarily of polytetrafluoroethylene (PTFE) was used. The contact angle between the electrode on the water surface and the water surface was 115° [27]. A previous study focused on the discharge characteristics of perpendicular electrodes on the water surface [28]. The present study investigates the electric field distribution and discharge characteristics of both parallel and perpendicular electrode models on the water surface.

Electric Field Distribution

The electric field distributions of the parallel and perpendicular electrode models were simulated using the MAXWELL 3D® simulation software. In the simulation, the outer diameter of the electrodes was 2 mm, the diameter of the conductor was 1.6 mm, and the horizontal spacing between the centers of the electrodes was 4 mm. The water bulk

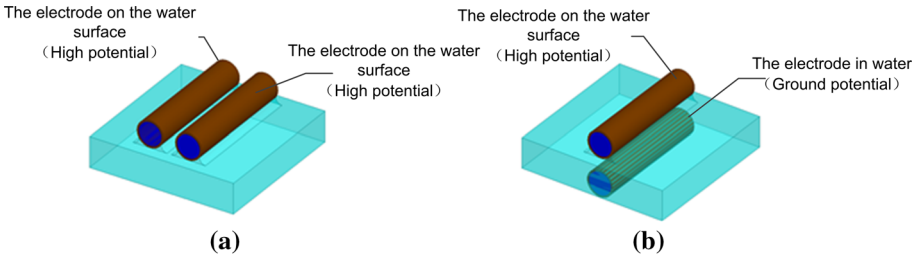

Fig. 1 Structural diagram of the electrode laboratory model **a** parallel electrode model **b** perpendicular electrode model

conductivity during simulation is 0.01 S/m. The relative permittivity of water during simulation is 81. When a high potential (4 kV) was applied to the two electrode models as shown in Fig. 2, the maximum electric field strength of the gas gap in the models was obtained. The strong electric field area, where the electric field strength exceeded a certain value ($E \geq 3 \times 10^6$ V/m), was obtained from Fig. 2 using the Adobe Photoshop software [29, 30]. That is, the area in which the electric field strength exceeded that value was assumed to be the plasma generation area [31, 32]. The maximum electric field strength and strong electric field area are shown in Table 1.

Table 1 and Fig. 2 show that the maximum electric field strength of the parallel electrode model was slightly smaller than that of the perpendicular electrode model; the reason is that the two electrodes in the parallel electrode model were arranged on the water surface and influenced each other. However, the perpendicular electrodes placed in water did not have a gas gap; therefore, the strong electric field area was considerably less than that of the parallel electrode model.

Discharge Characteristics

In this study, a sine-wave power supply with a frequency of 5–60 kHz and an output voltage of 0 to ±10 kV was adopted. A schematic diagram of the main discharge circuit is shown in Fig. 3 [27]. A resistance R2 is connected in series in the circuit. According to the Ohm's law, the discharge current is obtained by measuring the voltage on the resistance R2. In the experiment, the voltage was increased slowly, and we assume that when the discharge current occurred, the voltage was the initial discharge voltage. The experiment indicated that the initial discharge voltage of the parallel electrodes was 3.7 kV, and that of the perpendicular electrodes was 3.5 kV. The voltage was increased to 6 kV, and a snapshot of the discharge phenomena at an exposure time of 500 ms is shown in Fig. 4. The Fig. 4 is the discharge top view of the two electrode structures. The discharge voltage–current waveforms are shown in Fig. 5.

It can be concluded from Fig. 4 that a large stable plasma area was generated in both electrode models. However, the discharge areas of the two models were different. The discharge area of the parallel electrodes was larger than that of the perpendicular electrodes. From Fig. 5, it is clear that the instantaneous short pulse current of the parallel electrodes was greater than that of the perpendicular electrodes. This suggests that the plasma generation area of the parallel electrodes was much larger. The discharge

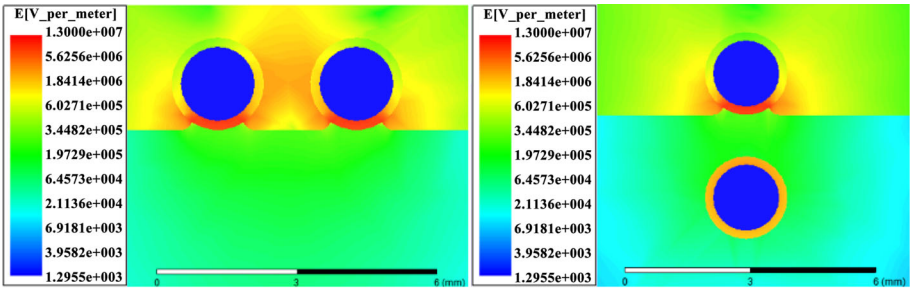

Fig. 2 Simulated electric field distribution diagram **a** parallel electrode model **b** perpendicular electrode model

Table 1 Electric field simulation results for the two electrode models

	Maximum electric field strength (V/m)	Strong electric field area (mm^2)
Parallel electrode model	7.551×10^6	1.39
Perpendicular electrode model	9.586×10^6	0.64

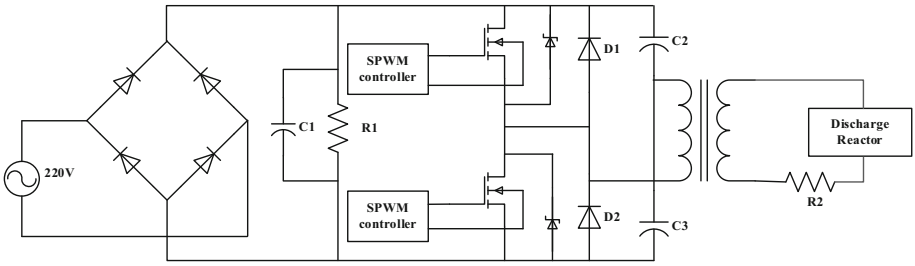

Fig. 3 Main discharge circuit

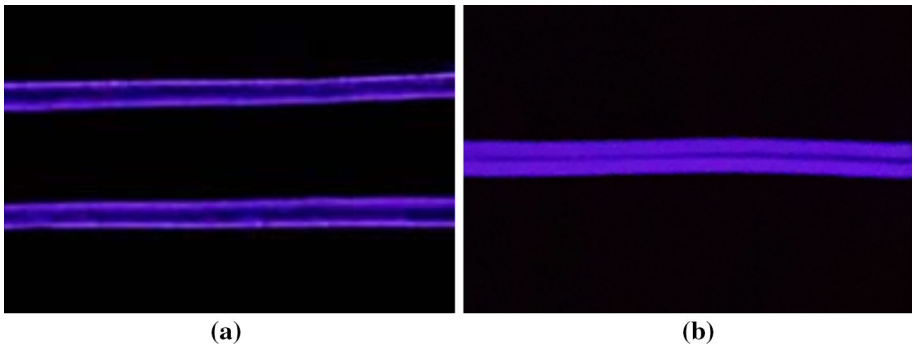

Fig. 4 Plasma discharge phenomenon under voltage of 6 kV **a** parallel electrode model **b** perpendicular electrode model

phenomenon in which the discharge is generally considered the diffusion type, with a discharge current on the order of milliamps, is known as a glow discharge. Other studies have used a strict definition of glow discharge in which there is only one discharge process in both the positive and negative half-cycles of an alternating current, and there is only one peak in the current waveform. The discharge form in which many discharges are generated in a half-cycle is called a glow-like discharge. However, the glow discharge was generated by a nanosecond pulse power, and the duration of each glow discharge was short, similar to that of several discharges in a half-cycle. Therefore, the current magnitude, and in particular the current density, was the main basis for defining this as a glow discharge. As seen in Fig. 5, several instantaneous short pulse currents appear in the half-cycle of voltage in the discharge voltage–current waveform of the two electrode models. The discharge currents of the parallel electrode and perpendicular electrode models were $\sim$18 and 8 mA,

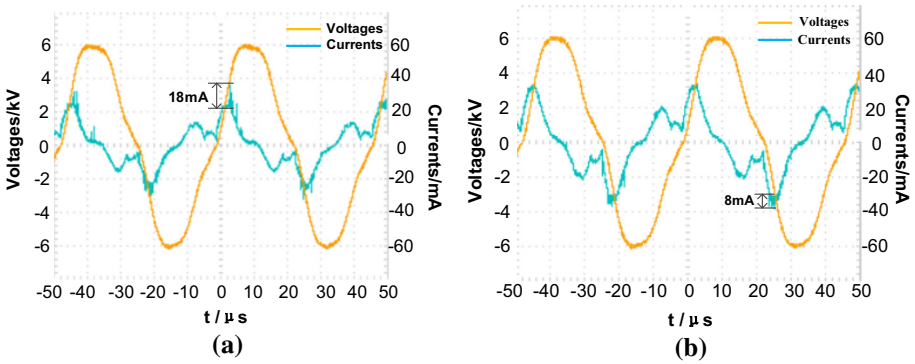

Fig. 5 Change in discharge voltage and current with time under voltage of 6 kV **a** parallel electrode model **b** perpendicular electrode model

respectively, fitting the current characteristics of a glow discharge. Therefore, the discharge form of the two electrode models could be conceptually considered a glow discharge or glow-like discharge.

Immersion Depth

The outer diameter of the electrodes was 2 mm, and they were spaced at a distance of 3 mm between their centers. The electric field simulation results for various immersion depths of the electrodes are shown in Fig. 6, and Table 2 lists the electric field parameters for different immersion depths.

From Fig. 6 and Table 2, it is clear that as the immersion depth increased, the angle of the gas gap between the electrode and the water surface gradually increased and the maximum electric field strength decreased. Therefore, when the electrodes were tangential to the water surface, the initial discharge voltage decreased to the minimum, and a larger plasma area was generated. The contact area between the generated active particles and the liquid surface was larger, and the treatment was more effective.

Horizontal Distance

The outer diameter of the electrodes was 2 mm. The electric field results of simulations in which the horizontal distance between the two electrodes was varied are shown in Fig. 7, and Table 3 lists the discharge parameters for parallel electrodes with different horizontal distances.

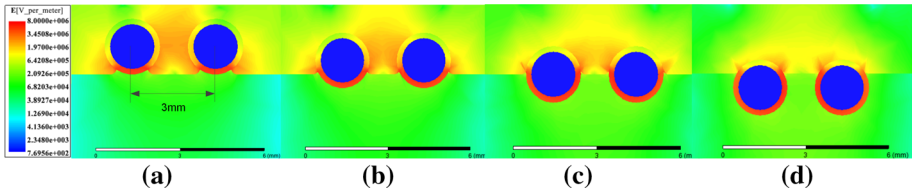

Fig. 6 Electric field simulation for different immersion depths **a** 0 mm, **b** 0.5 mm, **c** 1.0 mm and **d** 1.5 mm

Table 2 Electric field parameters for different immersion depths of electrode on water surface

Immersion depth (mm)	Maximum electric field strength (V/m)	Strong electric field area (mm^2)
0	7.5506×10^6	1.39
0.5	7.4011×10^6	0.87
1.0	7.2178×10^6	0.56
1.5	5.5574×10^6	0.18

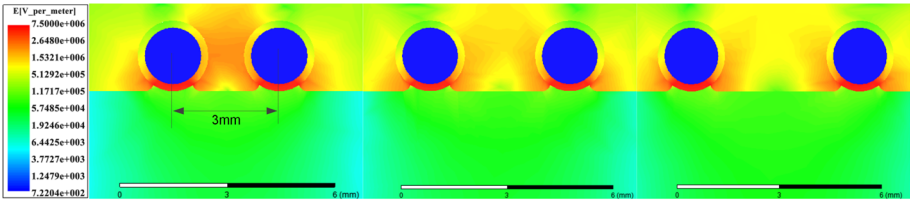

Fig. 7 Electric field simulation results for different horizontal distances **a** 3 mm, **b** 4 mm and **c** 5 mm

Table 3 Discharge parameters for different horizontal distances

Horizontal distance (mm)	Maximum electric field strength (V/m)	Initial discharge voltage (kV)
3	7.5664×10^6	3.9
4	8.0589×10^6	3.8
5	6.6204×10^6	4.0

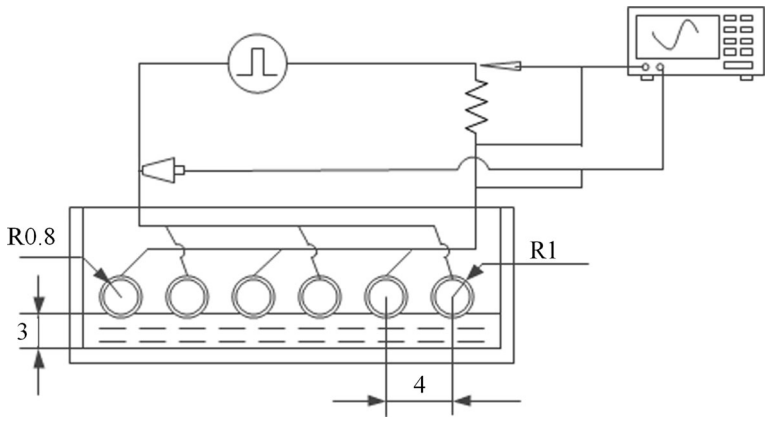

Fig. 8 Structural diagram of the plasma reactor

As seen in Fig. 7 and Table 3, when the horizontal distance was 4 mm, the maximum electric field strength was the largest. Whether or not the horizontal spacing increased, the power line cannot have a maximum concentration in the gas gap, which implies that the maximum electric field strength of the arrangement was relatively low. Therefore, the initial discharge voltage is smaller when the horizontal distance of the electrodes was 4 mm than that when the distance is 3 or 5 mm. The discharge area for 4 mm distance is larger than the other two cases when the same voltage is applied to the electrodes. So the treatment was more effective for 4 mm distance.

Experimental Decoloration of Organic Solutions

The water treatment plasma reactor is shown in Fig. 8. The reactor is composed of a discharge power supply and cylindrical electrodes. The outer diameter of the electrodes was 2 mm, and the horizontal distance between them was 4 mm; the electrodes were tangential to the water surface, and the depth of the solution to be treated was 3 mm.

Examples of industrial wastewater include dyeing wastewater, chemical industrial wastewater, and coking wastewater [31, 32]. In this study, methyl orange and azobenzene solutions were selected as the sample solutions. The concentration of the methyl orange solution and the azobenzene solution were 10 mg/L, and the volume was 50 mL. Two solutions were at rest during processing, and the temperature of two solutions was 10 °C. Place the solution for 10 min after completing the plasma treatment and then the absorbance of the two solutions was tested using a UV spectrophotometer to evaluate the decoloration rate of the pending solutions according to the formula [20, 33].

$$Decoloration\ rate = \frac{A_0 - A_t}{A_0} \times 100\ \% \tag{1}$$

where A_0 is the absorbance of the initial solution, and A_t is the absorbance of the solution after treatment.

The absorption curves are different curves which can demonstrate the absorptive capacity of the Light-absorbing substance solution to different wavelengths of light. The absorption curves of the methyl orange solution at treatment times of 0, 5, 10, and 15 min are shown in Fig. 9a. The maximum absorption wavelength of the methyl orange solution

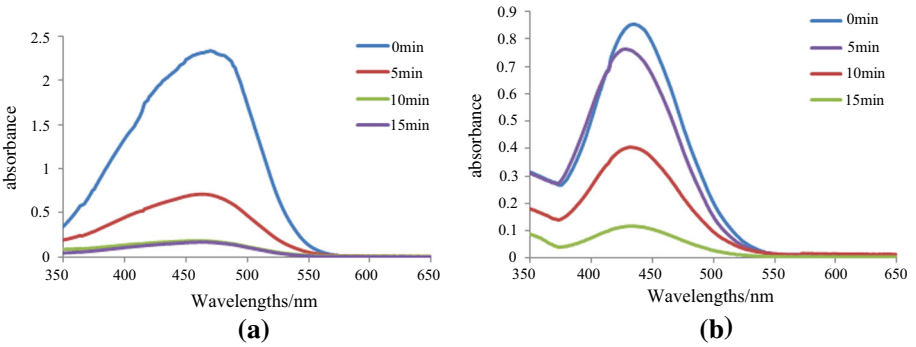

Fig. 9 Absorption *curves* of the methyl orange and azobenzene solutions **a** methyl orange solution **b** azobenzene solution

was 464 nm. With increasing treatment time, the absorbance of the methyl orange solution decreased. When the time was 15 min, the decoloration rate of the methyl orange solution was 93 %.

The absorption curves of the azobenzene solution at treatment times of 0, 5, 10, and 15 min are shown in Fig. 9b. The maximum absorption wavelength of the azobenzene solution was 431 nm. With increasing treatment time, the absorbance of the azobenzene solution decreased. When the time was 15 min, the decoloration rate of the azobenzene solution was 85 %.

The plasma contains a large number of free electrons, ions, neutral particles, and atoms and molecules in their excited states, as well as free radicals and so on. Because of the gas gap formed between the electrode and the water surface, a glow discharge occurs, and a large, stable plasma area is acquired for treating the wastewater surface. The methyl orange and azobenzene molecules react with many high-energy particles and strong oxidizing radicals (HO, HO_2, H_2O_2), breaking the bonds between organic molecules and opening the rings to form chain molecules. The generated chain molecules can further interact with the active particles. The ozone, free radicals, and other substances can oxidize and decompose pollutants to achieve the effect of decoloration. At the same time, the discharge process is accompanied by the effects of UV photolysis, supercritical water oxidation and so on. Finally, all of the above processes together degrade the two organic solutions to inorganic ions, water, and other compounds [34–36]. Because the pending solutions were maintained in a stationary state during the treatment, the organic molecules in the solution diffused with increasing treatment time.

Conclusions

The glow discharge plasma treatment of wastewater was presented in this paper. The electrode models for the method were discussed and analyzed by simulations and experiments. The conditions for generating a uniform and stable glow discharge plasma at the water surface in atmospheric pressure air were explored. Moreover, a methyl orange solution and an azobenzene solution were treated using the plasma reactor. The following conclusions were drawn:

(1) The electric field distribution and discharge characteristics of parallel electrode and perpendicular electrode models were compared. The glow discharge by the perpendicular electrode model was obtained at a low applied voltage, and a larger glow discharge area was generated by the parallel electrode model.
(2) The field strength of the gas gap can be affected by various factors such as the immersion depth of the parallel electrodes and the horizontal distance between them. A suitable electrode layout can sharply reduce the discharge voltage and result in a steady large plasma area, achieving more effective wastewater treatment.
(3) A methyl orange solution and an azobenzene solution were treated by the plasma reactor. The decoloration rates of the two organic solutions were 93 and 85 %, respectively, after 15 min

As the above conclusions demonstrate, the electrode structure we designed can generate a glow discharge plasma at the water surface in an atmospheric pressure air environment and can be used in industrial wastewater treatment. Thus, this study provides a new method for plasma water treatment.

References

1. Bozzi A, Yuranova T, Lais P, Kiwi J (2005) Degradation of industrial waste waters on fe/c-fabrics. Optimization of the solution parameters during reactor operation. Water Res 39:1441–1450
2. Figueira V, Vaz I (2011) Diversity and antibiotic resistance of *Aeromonas* spp. in drinking and waste water treatment plants. Water Res 45:5599–5611
3. Soares A, Guieysse B, Jefferson B, Cartmell E, Lester JN (2008) Nonylphenol in the environment: a critical review on occurrence, fate, toxicity and treatment in wastewaters. Environ Int 34:1033–1049
4. Catalkaya EC, Kargi F (2007) Color, toc and aox removals from pulp mill effluent by advanced oxidation processes: a comparative study. J Hazard Mater 139:244–253
5. Homlok R, Takács E, Wojnárovits L (2013) Degradation of organic molecules in advanced oxidation processes: relation between chemical structure and degradability. Chemosphere 91:383–389
6. Pera-Titus M, García-Molina V, Baños MA, Giménez J, Esplugas S (2004) Degradation of chlorophenols by means of advanced oxidation processes: a general review. Appl Catal B 47:219–256
7. Mahamuni NN, Adewuyi YG (2010) Advanced oxidation processes (aops) involving ultrasound for waste water treatment: a review with emphasis on cost estimation. Ultrason Sonochem 17:990–1003
8. Martinez-Huitle CA, Ferro S (2006) Electrochemical oxidation of organic pollutants for the wastewater treatment: direct and indirect processes. Cheminform 35:1324–1340
9. Carrier M, Besson M, Guillard C, Gonze E (2009) Removal of herbicide diuron and thermal degradation products under catalytic wet air oxidation conditions. Appl Catal B 91:275–283
10. Arena F, Italiano C, Raneri A, Saja C (2010) Mechanistic and kinetic insights into the wet air oxidation of phenol with oxygen (cwao) by homogeneous and heterogeneous transition-metal catalysts. Appl Catal B 99:321–328
11. Jing G, Al-Dahhan M (2005) Catalytic wet air oxidation of phenol in concurrent downflow and upflow packed-bed reactors over pillared clay catalyst. Chem Eng Sci 60:735–746
12. Lam SW, Chiang K, Lim TM, Amal R, Low KC (2005) The role of ferric ion in the photochemical and photocatalytic oxidation of resorcinol. J Catal 234:292–299
13. Mikkel WN, HGdall EV, Elena M, HGdall CK, Christian S, Heegaard NHH (2005) Sample handling for mass spectrometric proteomic investigations of human sera. Anal Chem 77:5114–5123
14. Konhauser KO, Amskold L, Lalonde SV, Posth NR, Kappler A, Anbar A (2007) Decoupling photochemical Fe(ii) oxidation from shallow-water bif deposition. Earth Planet Sci Lett 258:87–100
15. Foster J, Sommers BS, Gucker SN, Blankson IM, Adamovsky G (2012) Perspectives on the interaction of plasmas with liquid water for water purification. Plasma Sci IEEE Trans 40:1311–1323
16. Narengerile, Watanabe T (2012) Acetone decomposition by water plasmas at atmospheric pressure. Chem Eng Sci 69:296–303
17. Peng JW, Lee S (2013) Atmospheric pressure plasma degradation of azo dyes in water: PH and structural effects. Plasma Chem Plasma Process 33:1063–1072
18. Hayes J, Kirf D, Garvey M, Rowan N (2013) Disinfection and toxicological assessments of pulsed UV and pulsed-plasma gas-discharge treated-water containing the waterborne protozoan enteroparasite cryptosporidium parvum. J Microbiol Methods 94:325–337
19. Nikiforov AY (2009) An application of ac glow discharge stabilized by fast air flow for water treatment. Plasma Sci IEEE Trans 37:872–876
20. Liu Y, Mei S, Djakaou IS, Simeon C, Stephanie O (2012) Carbamazepine removal from water by dielectric barrier discharge: comparison of ex situ and in situ discharge on water. Chem Eng Process 56:10–18
21. Mok YS, Jo JO (2006) Degradation of organic contaminant by using dielectric barrier discharge reactor immersed in wastewater. Plasma Sci IEEE Trans 34:2624–2629
22. Zhang Q, Liang Y, Feng H, Ma R, Tian Y, Zhang J et al (2013) A study of oxidative stress induced by non-thermal plasma-activated water for bacterial damage. Appl Phys Lett 102:203701–203701-4
23. Gao L, Sun L, Wan S, Yu Z, Li M (2013) Degradation kinetics and mechanism of emerging contaminants in water by dielectric barrier discharge non-thermal plasma: the case of 17β-estradiol. Chem Eng J 228:790–798
24. Choi S, Watanabe T (2012) Decomposition of 1-decanol emulsion by water thermal plasma jet. Plasma Sci IEEE Trans 40:2831–2836
25. Mok YS, Ahn HT, Kim JT (2007) Treatment of dyeing wastewater by using positive pulsed corona discharge to water surface. Plasma Sci Technol 9:71–75
26. Du S, Xu J, Mi J, Li N (2012) Study on earthed atomizing corona discharge enhancing the biodegradability of waste water from oil extraction. Eur Phys J Appl Phys 59:994–1000
27. Chibowski E (2007) On some relations between advancing, receding and young's contact angles. Adv Colloid Interface Sci 133:51–59

28. Wenzheng L, Chuanhui L (2014) Study on the generation characteristics of dielectric barrier discharge plasmas on water surface. Plasma Sci Technol 16:26–31
29. Boussaton MP, Coquillat S, Chauzy S, Georgis JF (2005) Influence of water conductivity on micro-discharges from raindrops in strong electric fields. Atmos Res 76:330–345
30. Macheret SO, Shneider MN, Murray RC (2006) Ionization in strong electric fields and dynamics of nanosecond-pulse plasmas. Phys Plasmas (1994-present) 13:391–400
31. Ivanov SN, Lisenkov VV (2010) Evolution of subnanosecond pulsed electric breakdown of gas gaps for uniform gas preionization. Tech Phys 55:53–57
32. Bo HE, Zhang G, Chen BF, Gao NK, Yaozhong LI (2010) The influence of the sand-dust environment on air-gap breakdown discharge characteristics of the plate-to-plate electrode. Sci China Phys Mech Astron 53(3):458–464
33. Abdullah FH, Rauf MA, Ashraf SS (2007) Kinetics and optimization of photolytic decoloration of carmine by UV/H_2O_2. Dyes Pigments 75:194–198
34. Lu D, Chen J, Gao A, Zissis G, Hu S, Lu Z (2010) Decolorization of aqueous acid red b solution during the cathode process in abnormal glow discharge. Plasma Sci IEEE Trans 38(10):2854–2859
35. Jin X, Bai H, Wang F, Wang X (2011) Plasma degradation of acid orange 7 with contact glow discharge electrolysis. IEEE Trans Plasma Sci 39(4):1099–1103
36. Narengerile, Saito H, Watanabe T (2010) Decomposition mechanism of fluorinated compounds in water plasmas generated under atmospheric pressure. Plasma Chem Plasma Process 30(6):813–829